NUCL SCI TECH (2018) 29:131
https://doi.org/10.1007/s41365-018-0470-5

Mechanical-force-promoted peptide assembly: a general method

Yue Yuan[1,2] · Qi-Qi-Ge Du[2,3] · Yu-Jiao Wang[2] · Jun Hu[2] · Shi-Tao Lou[1] · Yi Zhang[2]

Received: 11 January 2018 / Revised: 5 March 2018 / Accepted: 19 March 2018 / Published online: 27 July 2018

Abstract A general method was developed for promoting peptide assembly and protein polymerization to form nanoscale patterns on various surfaces with an atomic force microscope (AFM) operated in a liquid. By scanning solid surfaces with an AFM tip, we showed that peptide monomers assemble at a higher rate in the tip-scanned area compared to other regions. The promotion is attributed to the mechanical force applied by the scanning tip. This kind of mechanical-force-promoted assembly was also observed with different peptides on various substrates. The force promoting peptide assembly provides a simple and practical solution for preparing and building peptide and protein architectures for future nanodevices.

This work was supported by the National Natural Science Foundation of China (No. 11674344), the National Basic Research Program of China (973 program, No. 2013CB932801), and the Key Research Program of Frontier Sciences, Chinese Academy of Sciences (No. QYZDJ-SSW-SLH019-2).

✉ Yue Yuan
18817393143@163.com

Shi-Tao Lou
stlou@admin.ecnu.edu.cn

Yi Zhang
zhangyi@sinap.ac.cn

[1] State Key Laboratory of Precision Spectroscopy, East China Normal University, Shanghai 200062, China

[2] Key Laboratory of Interfacial Physics and Technology, Shanghai Institute of Applied Physics, Chinese Academy of Sciences, Shanghai 201800, China

[3] School of Life Sciences, Inner Mongolia Agricultural University, Hohhot 010018, China

Keywords Self-assembly · Peptide · Nanomechanical stimulus · Support lipid bilayers · Atomic force microscope

1 Introduction

Self-assembly is one of the most important mechanisms that nature exploits to build complex structures. Particularly, self-assembly of peptides and proteins is one of the few practical strategies for making ensembles of nanostructures, is common to numerous dynamic multicomponent systems, from smart materials and self-healing structures to sensors [1–3], and has received considerable attention in the areas of nanochemistry and biomedical engineering [4, 5]. To this end, great effort has been devoted to controlling the peptide and protein self-assembly processes to develop periodic nanostructured patterns [6–9]. The mechanical force applied by an atomic force microscope (AFM) tip has been used to induce the self-assembly of peptides and proteins at water–solid interfaces [6, 10–17]. However, the generality of this method remains unclear.

In this paper, Pep11 (NH_2–Gln–Gln–Arg–Phe–Gln–Trp–Gln–Phe–Glu–Gln–Gln–NH_2), an artificially synthesized peptide [18], and actin, one of the main cytoskeleton proteins of cells [19], were employed as examples and assembled on a bare mica surface and lipid-decorated mica substrate, respectively. Both surfaces are smooth and hydrophilic and should be quite different from polymer-coated mica substrates [20–22]. Results from the two quite different peptides indicate it is a general phenomenon that mechanical force applied by an AFM tip promotes peptide self-assembly.

2 Materials and methods

Lipids DOPC (1,2-dioleoyl-sn-glycero-3-phosphocholine), DOTAP (1,2-dioleoyl-3-trimethylammonium-propane), DPPC (1,2-dipalmitoyl-sn-glycero-3-phocholine), and EDPPC (16:0) (1,2-dipalmitoyl-sn-glycero-3-ethylphosphocholine, positively charged) were purchased from Avanti Polar Lipids (Alabaster, AL). All the lipids were dissolved in chloroform at 5 mg/ml. The peptide termed as Pep11 with purity 98.3% was custom-synthesized by China Peptides. Purified G-actin (monomer) from rabbit skeletal muscle with purity > 99% was purchased from Cytoskeleton Inc. (USA). The G-actin powder was used as received without further purification. ATP and guanidine carbonate were purchased from Sigma. Other chemicals were bought from China Chemicals Ltd., Inc. All chemicals were of chemical grade and used as received without further purification.

2.1 Preparation of Pep11

The Pep11 powder was dissolved in 10 mM PBS (phosphate 10 mM, NaCl 20 mM, pH 7.0) to a certain concentration. Then, the solutions were centrifuged on a centrifuge (Hitachi, Japan) at a rate of 12,000 rpm for 20 min to eliminate the possible aggregates, and the supernatant was immediately used in the experiment.

2.2 Preparation of actin

G-Actin was dissolved to a concentration of 10 mg/ml in Tris-HCl buffer (pH 8.0, 5 mM) containing 0.2 mM $CaCl_2$, 0.2 mM ATP, and 5% (w/v) sucrose. Then, the G-actin solution was quickly frozen in liquid nitrogen and stored at − 80 °C. Before experiments, the prepared G-actin solution was diluted to 0.4 mg/ml with general actin buffer (GB), which consisted of 5 mM Tris-HCl (pH 8.0), 0.2 mM $CaCl_2$, 0.2 mM ATP, and 0.5 mM DTT. The diluted G-actin solution was incubated on ice for 60 min to depolymerize possibly existing actin oligomers, which might form during storage. After that, the solution was centrifuged in a 4 °C microfuge tube at 14,000 rpm for 30 min to remove any large actin crystals generated by the snap-freezing process. Then, the supernatant was transferred to a new microfuge tube and further diluted with GB to a desired working concentration for experiments. F-actin was polymerized from G-actin by addition of polymerization buffer (PB), which was made up of 100 mM Tris-HCl (pH 7.5), 20 mM $MgCl_2$, 500 mM KCl, 50 mM guanidine carbonate, and 10 mM ATP.

2.3 Formation of supported lipid bilayers (SLBs)

The SLBs were formed by the vesicle rupture method [23–26]. An appropriate amount of a phospholipid chloroform solution was placed into a small vessel, and the chloroform was removed using a stream of dry nitrogen. The dry phospholipid was then resuspended in pure water to its final concentration of 0.5 mg/ml and sonicated at room temperature until the solution appeared to be clear. Next, 100 μL of the solution was deposited on freshly cleaved pure mica ($KAl_2(Si_3AlO_{10})(OH)_2$, 1 cm × 1 cm, Sichuan Meifeng Co., China). If the lipid samples had phase transition temperature above 25 °C, they were incubated in a sealed humid chamber within a heater at 60 °C for 30 min. Otherwise, the lipid samples were incubated at room temperature. After a controlled period of time, the samples were gently rinsed with pure water to remove any lipids weakly attached to the substrate and remaining in solution. Rinsing involved ten repeated washes, each with approximately 100 μL of purified water from a pipette. The prepared SLBs were then carefully inserted into an AFM.

2.4 AFM study

AFM operations were conducted on a commercial Multimode AFM system (Multimode 8, Bruker) equipped with a liquid cell and J-scanner. Oxide-sharpened silicon nitride cantilevers (Bruker) with typical spring constants of 0.32 N/m were used. The AFM was operated in tapping mode or Peak Force Tapping Mode with loading ranging from 50 to 400 pN depending on different substrates and peptides [13, 27].

3 Results and discussion

3.1 Mechanical-force-promoted peptide self-assembly on mica

Pep11 contains two hydrophilic amino acid residues (Arg and Glu), which can be oppositely charged and provide strong electrostatic interaction during peptide assembly [18]. Peptide Pep11 was first deposited onto a negatively charged mica surface in an aqueous solution [28, 29]. In situ AFM scanning was then used to apply a mechanical force of piconewton-to-nanonewton levels to the sample on the mica surface and to monitor the force-induced peptide assembly in real time. The mechanical force applied by the AFM tip was manipulated by adjusting the tip oscillation amplitude and setpoint [13]. Figure 1 illustrates the self-assembly of Pep11 (0.9 mg/mL) during

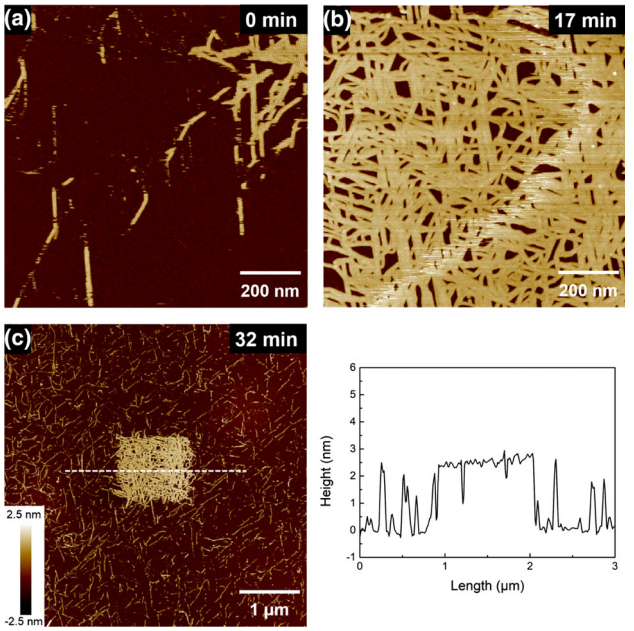

Fig. 1 (Color online) AFM topological images of Pep11 peptide nanofibers formed on a bare mica substrate. **a** After the first tapping-mode scan of the substrate by the AFM tip. **b** Pep11 nanofibers almost covered the whole area after continuous scanning of the same area by the AFM tip four times. **c** A zoomed-out image indicating the promoting effect of AFM scanning on peptide assembly (left) and section analysis of the white dashed line (right)

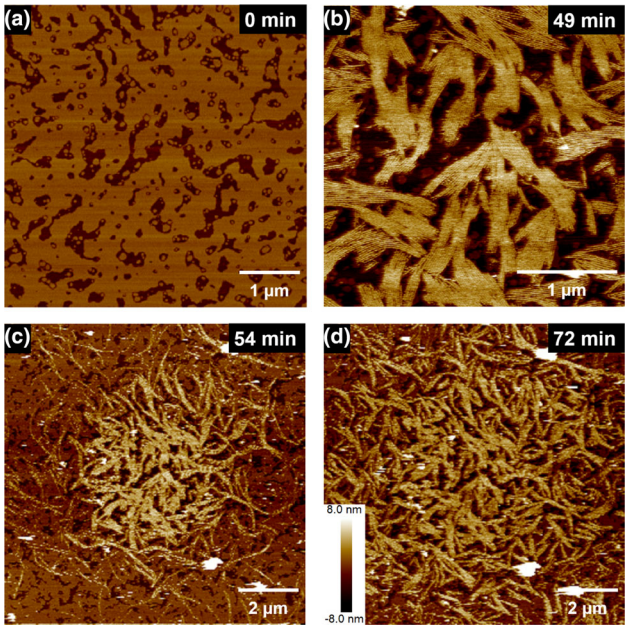

Fig. 2 (Color online) Tapping-mode AFM images indicating the polymerization of G-actin on a specific substrate of the 4:1 DOPC/DOTAP fluid-phase lipid bilayer. **a** An AFM image of a 4:1 DOPC/DOTAP cationic fluid-phase lipid bilayer. **b** Mechanical-force-promoted polymerization of G-actin into F-actin on the lipid bilayer. **c** A zoomed-out AFM image indicating that F-actin was mostly present in the tip-scanned area. **d** Actin continued to grow and filled the entire area after a further scan by the AFM tip in the next 18 min

scanning by an AFM tip in tapping mode in PBS. First, several Pep11 nanofibers appeared on the substrate after first scanning over the area of 1 μm × 1 μm (Fig. 1a). Then, the nanofibers covered almost the whole scanning area after four subsequent scans (Fig. 1b). AFM analysis of a zoomed-out image (Fig. 1c) indicates that the formed peptide fibers have a height of ∼ 2.5 nm. It is clear that the AFM scans greatly promoted Pep11 self-assembly because of the strong contrast between the scanned area and peripheral regions. Therefore, AFM scanning is a crucial factor for inducing and accelerating Pep11 self-assembly on a mica surface and can be used to fabricate patterns with specific shapes at desired locations.

3.2 Mechanical-force-promoted polymerization of G-actin on SLBs

In addition to the mechanical-force-promoted peptide self-assembly on the bare mica, the mechanical force also has an effect on actin polymerization on SLBs. G-Actin polymerizes into F-actin faster under a scanning AFM tip on 4:1 DOPC/DOTAP bilayers. An AFM image (Fig. 2a) indicates that a fluid-phase bilayer, 4:1 DOPC/DOTAP, has a height of 5 nm on the mica substrate. After addition of G-actin (∼ 20 μg/ml) into the system, G-actin tended to polymerize into F-actin on the bilayers and to spread to the whole imaging area to form a densely packed pattern in the next 50 min (Fig. 2b) during continuous scanning by the AFM tip in tapping mode. Interestingly, although the SLBs were in the fluid phase and thus could move around on the substrate, the formed actin fibers were stable at least for hours during the scanning by the AFM tip. In addition, it was found that G-actin polymerized into fibers without the help of polymerization buffer, which was normally required. This phenomenon may be ascribed to the cationic lipid DOTAP (present in the SLBs), which may facilitate the deposition and polymerization of negatively charged G-actin on the SLBs. When the AFM imaging was zoomed out to a large area, it was found that most of the actin fibers were located at the center of the new image (Fig. 2c). Thus, it is clear that continuous scanning by the AFM tip in tapping mode accelerated the polymerization of G-actin into F-actin on the fluid-phase bilayer.

To validate the impact of the mechanical force on the actin polymerization on more specific surfaces, SLBs composed of gel-phase lipids at room temperature were examined. Bilayers of 80% DPPC and 20% EDPPC were formed at 60 °C and cooled to room temperature (Fig. 3a). Figure 3b shows the closely packed F-actin formed on the cationic gel-phase lipid bilayer after scanning of the same area by the AFM tip for 106 min at a G-actin concentration

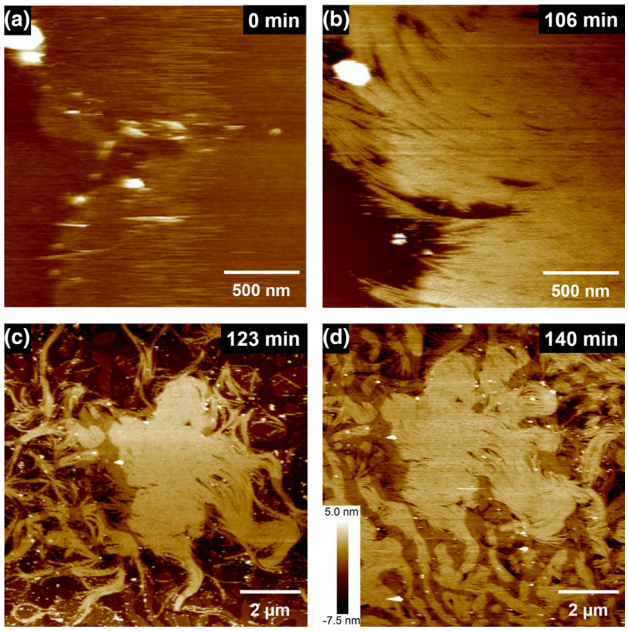

Fig. 3 (Color online) Tapping-mode AFM images indicating that F-actin formed on a 4:1 DPPC/EDPPC cationic gel-phase lipid bilayer. **a** An image of SLBs just after addition of G-actin into the system. **b** A large amount of F-actin formed after a continual scan by the AFM tip for 106 min. **c** A zoomed-out image indicating that F-actin was mostly formed in the area that was previously scanned by the AFM tip. **d** An AFM image indicating that F-actin continued to grow and filled the entire area. Images were obtained with a very small load to avoid disassembling the formed actin fibers on the substrate

of $\sim$ 20 μg/ml. In a zoomed-out image, we can see that F-actin grew from the previously scanned area (Fig. 3c) and quickly covered almost the entire area (Fig. 3d). The fast expanding actin fibers during AFM scanning indicated a strong effect of the AFM nanomechanical stimulus on the self-assembly of G-actin.

The above results suggested that AFM tip scanning of the substrate facilitated the actin assembly. Because the AFM tip was scanning the surface in oscillating mode in the Z-direction and back and forth laterally, actin monomers should be mechanically pushed around on the substrate, and this action should increase the probability of interaction with other monomers to form a trimer that is necessary to start polymerization. The phase of the lipid bilayers also played a role in the actin polymerization. It was found that the fluid-phase bilayers took less time to form actin fibers than did gel-phase bilayers even under the same AFM scanning conditions. This result may be due to the fact that fluid-phase bilayers have lower lipid density and faster lipid flip-flop rates than do gel-phase bilayers, and these properties helped G-actin to interact with other monomers. Be that as it may, we presented a method for site-specific creation of a stable F-actin network on lipid membranes.

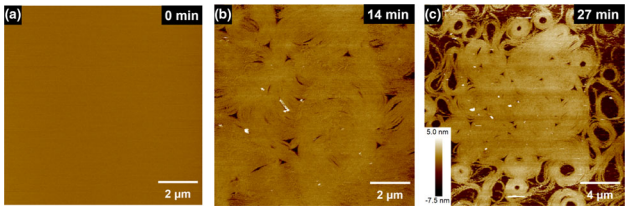

Fig. 4 (Color online) Tapping-mode AFM images indicating the deposition of F-actin on the 4:1 DOPC/DOTAP lipid bilayer as promoted by the scanning tip. **a** The smooth lipid bilayer. **b** The same area after addition of 40 μg/ml F-actin. The AFM tip continuously scanned this area for $\sim$ 4 min. **c** A zoomed-out image of the deposited F-actin

3.3 Mechanical-force-promoted deposition of F-actin on SLBs

An F-actin solution was placed onto the 4:1 DOPC/DOTAP bilayers to check the AFM tip effect on the deposition of prepolymerized F-actin on lipid membranes. AFM imaging indicated that the preformed actin fibers deposited and continued to elongate on the bilayers (Fig. 4). This result indicates that the mechanical stimulus promotes deposition of F-actin on SLBs.

4 Conclusion

In this paper, we examined the effects of a mechanical-force stimulus on the self-assembly of peptide Pep11 and actin on either bare mica or SLBs. By applying a force with a scanning AFM tip, we proved that Pep11 and actin assemble faster on various substrates. We demonstrated that nanoscale patterns of peptides and proteins could be created by means of an AFM tip to apply a mechanical force during peptide assembly. Our method turned out to be a simple but general solution for preparing and building peptide and protein architectures for future nanodevices.

References

1. K. Channon, C.E. MacPhee, Possibilities for 'smart' materials exploiting the self-assembly of polypeptides into fibrils. Soft Matter **4**, 647 (2008). https://doi.org/10.1039/b713013a
2. F. Gelain, D. Silva, A. Caprini et al., BMHP1-derived self-assembling peptides: hierarchically assembled structures with self-healing propensity and potential for tissue engineering applications. ACS Nano **5**, 1845–1859 (2011). https://doi.org/10.1021/nn102663a
3. C.A. Hauser, S. Zhang, Designer self-assembling peptide nanofiber biological materials. Chem. Soc. Rev. **39**, 2780–2790 (2010). https://doi.org/10.1039/b921448h
4. S. Zhang, Fabrication of novel biomaterials through molecular self-assembly. Nat. Biotechnol. **21**(10), 1171–8 (2003). https://doi.org/10.1038/nbt874

5. G.R. Heath, B.R. Johnson, P.D. Olmsted et al., Actin assembly at model-supported lipid bilayers. Biophys. J. **105**, 2355–65 (2013). https://doi.org/10.1016/j.bpj.2013.10.007
6. J. Chang, X.F. Peng, K. Hijji et al., Nanomechanical stimulus accelerates and directs the self-assembly of silk-elastin-like nanofibers. J. Am. Chem. Soc. **133**, 1745–7 (2011). https://doi.org/10.1021/ja110191f
7. T. Kudernac, S. Lei, J.A. Elemans et al., Two-dimensional supramolecular self-assembly: nanoporous networks on surfaces. Chem. Soc. Rev. **38**, 402–21 (2009). https://doi.org/10.1039/b708902n
8. K.L. Christman, V.D. Enriquez-Rios, H.D. Maynard, Nanopatterning proteins and peptides. Soft Matter **2**, 928 (2006). https://doi.org/10.1039/b611000b
9. T. Gan, B. Wu, X. Zhou et al., Ultrahigh resolution, serial fabrication of three dimensionally-patterned protein nanostructures by liquid-mediated non-contact scanning probe lithography. RSC Adv. **6**, 50331–50335 (2016). https://doi.org/10.1039/c6ra07715c
10. G.K. Binnig, C.F. Quate, C. Gerber, Atomic force microscope. Phys. Rev. Lett. **56**, 930–933 (1986). https://doi.org/10.1103/PhysRevLett.56.930
11. O. Custance, R. Perez, S. Morita, Atomic force microscopy as a tool for atom manipulation. Nat. Nanotechnol. **4**, 803–10 (2009). https://doi.org/10.1038/nnano.2009.347
12. R. Garcia, A.W. Knoll, E. Riedo, Advanced scanning probe lithography. Nat. Nanotechnol. **9**, 577–87 (2014). https://doi.org/10.1038/nnano.2014.157
13. X. Zhang, X. Hu, H. Lei et al., Mechanical force-induced polymerization and depolymerization of F-actin at water/solid interfaces. Nanoscale **8**, 6008–6013 (2016). https://doi.org/10.1039/C5NR08713A
14. A.S. Lea, A. Pungor, V. Hlady et al., Manipulation of proteins on mica by atomic force microscopy. Langmuir **8**, 68–73 (1992). https://doi.org/10.1021/la00037a015
15. H. Yang, S. Fung, M. Pritzker et al., Mechanical force induced nucleation and growth of peptide nanofibers at liquid/solid interfaces. Angew. Chem. **47**, 4397–4400 (2008). https://doi.org/10.1002/anie.200705404
16. A. Karsai, T.J. Slack, H. Malekan et al., Local mechanical perturbation provides an effective means to regulate the growth and assembly of functional peptide fibrils. Small **12**, 6407–6415 (2016). https://doi.org/10.1002/smll.201601657
17. J. Zhong, M. Ma, J. Zhou et al., Tip-induced micropatterning of silk fibroin protein using in situ solution atomic force microscopy. ACS Appl. Mater. Interfaces **5**, 737–46 (2013). https://doi.org/10.1021/am302271g
18. Q. Du, B. Dai, J. Hou et al., A comparative study on the self-assembly of an amyloid-like peptide at water–solid interfaces and in bulk solutions. Microsc. Res. Tech. **78**, 375–81 (2015). https://doi.org/10.1002/jemt.22483
19. W. Kabsch, J. Vandekerckhove, Structure and function of actin. Annu. Rev. Biophys. Biomol. Struct. **21**, 49–76 (1992). https://doi.org/10.1146/annurev.bb.21.060192.000405
20. M. Dong, S. Xu, C.L.P. Oliveira et al., Conformational changes in mannan-binding lectin bound to ligand surfaces. J. Immunol. **178**, 3016–3022 (2007). https://doi.org/10.4049/jimmunol.178.5.3016
21. A. Keller, M. Fritzsche, Y. Yu et al., Influence of hydrophobicity on the surface-catalyzed assembly of the islet amyloid polypeptide. ACS Nano **5**, 2770–2778 (2011). https://doi.org/10.1021/nn1031998
22. Q. Li, L. Liu, S. Zhang et al., Modulating Aβ33-42 peptide assembly by graphene oxide. Chem. Eur. J. **20**, 7236–7240 (2014). https://doi.org/10.1002/chem.201402022
23. M.-P. Mingeot-Leclercq, M. Deleu, R. Brasseur et al., Atomic force microscopy of supported lipid bilayers. Nat. Protoc. **3**, 1654–1659 (2008). https://doi.org/10.1038/nprot.2008.149
24. Z.V. Leonenko, E. Finot, H. Ma et al., Investigation of temperature-induced phase transitions in DOPC and DPPC phospholipid bilayers using temperature-controlled scanning force microscopy. Biophys. J. **86**, 3783–3793 (2004). https://doi.org/10.1529/biophysj.103.036681
25. H.Z. Lei, T. Tian, Q. Du et al., Sequence-dependent interactions between model peptides and lipid bilayers. Nucl. Sci. Tech. **28**, 124 (2017). https://doi.org/10.1007/s41365-017-0280-1
26. R.P. Richter, J.L.K. Him, A. Brisson, Supported lipid membranes. Mater. Today **6**, 32–37 (2003). https://doi.org/10.1016/s1369-7021(03)01129-5
27. S. Zhang, H. Aslan, F. Besenbacher et al., Quantitative biomolecular imaging by dynamic nanomechanical mapping. Chem. Soc. Rev. **43**, 7412–7429 (2014). https://doi.org/10.1039/C4CS00176A
28. C. Whitehouse, J. Fang, A. Aggeli et al., Adsorption and self-assembly of peptides on mica substrates. Angew. Chem. Int. Ed. Engl. **44**, 1965–8 (2005). https://doi.org/10.1002/anie.200462160
29. S. Nishimura, H. Tateyama, K. Tsunematsu et al., Zeta potential measurement of muscovite mica basal plane-aqueous solution interface by means of plane interface technique. J. Colloid Interface Sci. **152**, 359–367 (1992). https://doi.org/10.1016/0021-9797(92)90038-n